The Bioscan AN INTERNATIONAL QUARTERLY JOURNAL OF LIFE SCIENCES 20(3): 2008-2032,2025 www.thebioscan.com

Formulation Development and In-Vitro/In-Vivo Evaluation of Dual-Drug Lipid Nanoparticle Systems for Synergistic Amelioration of Cardiac Pathology in Type 2 Diabetes Mellitus

[1]A. Seetha Devi*

[1]Professor, Department of Pharmaceutics, Gokaraju Rangaraju College of Pharmacy, Bachupally, Hyderabad, Telangana. 500090

Email:- seethagottipati@gmail.com

Corresponding Authors

[1]A. Seetha Devi*

[1]Professor, Department of Pharmaceutics, Gokaraju Rangaraju College of Pharmacy, Bachupally, Hyderabad, Telangana. 500090

Email:- seethagottipati@gmail.com

DOI: 10.63001/tbs.2025.v20.i03.pp2008-2032

KEYWORDS
Lipid nanoparticles,co-delivery, diabetic cardiomyopathyoxidative stress,nanomedicine.

Received on:

30-09-2025

Acceptedon:

05-11-2025

Publishedon:

07-12-2025

Abstract

The study aimed to develop and evaluate co-loaded lipid nanoparticles (CL-LNPs) for synergistic management of type 2 diabetes–associated cardiomyopathy. The nanoparticles were prepared using a modified hot-emulsion ultrasonication method and characterized for particle size, polydispersity index, zeta potential, entrapment efficiency, and drug release behavior. The optimized CL-LNPs exhibited nanoscale dimensions with low PDI and a sufficiently negative surface charge, ensuring colloidal stability. Entrapment efficiency for both therapeutic agents remained high, and the sustained-release profile extended up to 48 hours. Antioxidant evaluation using DPPH, ABTS, and nitric oxide assays revealed significantly higher radical scavenging potential in CL-LNPs compared to free drugs and single-loaded formulations. Anti-inflammatory studies further demonstrated superior inhibition of protein denaturation and enhanced stabilization of human RBC membranes. Cytotoxicity assessment on H9c2 cardiomyocytes showed improved cell viability and reduced IC_{50} values for CL-LNPs, while intracellular ROS measurement and LDH leakage assays confirmed potent cytoprotective effects. Overall, the results indicate that co-loaded lipid nanoparticles provide a promising strategy for targeting oxidative stress, inflammation, and cellular injury in diabetic cardiomyopathy. The synergistic performance of dual-drug delivery highlights their potential for further in-vivo exploration and therapeutic translation.

INTRODUCTION

Type 2 diabetes mellitus (T2DM) has emerged as one of the most prevalent metabolic disorders worldwide, contributing significantly to morbidity

and mortality due to its long-term complications. Among these, diabetic cardiomyopathy represents a major cardiovascular consequence characterized by structural, functional, and metabolic abnormalities in the myocardium independent of hypertension or coronary artery disease. Prolonged hyperglycaemia in T2DM leads to oxidative stress, persistent inflammation, mitochondrial dysfunction, and accumulation of advanced glycation end products, which together accelerate myocardial remodelling, fibrosis, and eventual cardiac failure. As a result, diabetic cardiomyopathy has become a critical clinical challenge, requiring therapeutic strategies that can simultaneously address multiple pathological pathways rather than targeting a single mechanism. Conventional treatments such as antidiabetic drugs or antioxidants, although beneficial, often suffer from limitations including poor solubility, rapid degradation, poor permeability, and inadequate cardiac tissue targeting (Abdelsaid et al., 2016, Cryer et al., 2016, Karam et al., 2017, Wong et al., 2017).

In recent years, lipid-based nanocarriers have gained significant attention for improving drug delivery in chronic metabolic and cardiovascular diseases. Lipid nanoparticles, owing to their biocompatibility, biodegradability, and structural similarity to biological membranes, offer several advantages such as high drug-loading capability, enhanced stability of encapsulated agents, controlled release, and improved cellular uptake. These features are particularly useful for drugs that demonstrate poor solubility or limited bioavailability in conventional dosage forms. Moreover, co-encapsulation of more than one therapeutic agent in a single nanocarrier platform enables synergistic action, reduced dosing frequency, and the ability to modulate multiple molecular pathways concurrently. This is especially relevant for diabetic cardiomyopathy, where oxidative stress, inflammation, and cellular injury coexist and contribute to disease progression (Abdelsaid et al., 2016, Nakhate et al., 2016, Ighodaro et al., 2017, Bathina and Das, 2018, Bogdanov et al., 2018).

A combination therapy approach involving antioxidants and anti-inflammatory agents has been proposed as a promising strategy for attenuating myocardial dysfunction in T2DM.

However, free drugs often display suboptimal pharmacokinetics, rapid systemic elimination, and limited accumulation in cardiac tissues. Nanocarrier-based co-delivery systems can overcome these barriers by enhancing solubility, prolonging circulation time, protecting the cargo from degradation, and enabling sustained-release behavior. Lipid nanoparticles are particularly suitable for delivering lipophilic or moderately lipophilic therapeutic molecules, providing efficient encapsulation and intracellular retention. By maintaining therapeutic concentrations over an extended period, lipid nanoparticles may effectively mitigate oxidative and inflammatory insults associated with diabetic cardiomyopathy (Wong et al., 2017, Alwafi et al., 2020, Andrade et al., 2020, Arroyave et al., 2020, Arvanitakis et al., 2020, Avilés-Santa et al., 2020).

Despite growing interest in nanomedicine for metabolic and cardiovascular disorders, evidence supporting the use of co-loaded lipid nanoparticles for diabetic cardiomyopathy remains limited. Most studies have focused on single-drug-loaded systems or non-lipid-based carriers, leaving a significant research gap regarding the benefits of dual-drug lipid nanocarriers designed specifically for cardiac protection. In this context, the development of co-loaded lipid nanoparticles incorporating two complementary therapeutic agents offers a promising pathway for enhancing cardioprotection, reducing oxidative damage, and improving myocardial stability in T2DM (Wong et al., 2017, Alwafi et al., 2020, Andrade et al., 2020, Arroyave et al., 2020, Arvanitakis et al., 2020, Avilés-Santa et al., 2020).

In light of these considerations, the present study aimed to design, develop, and evaluate co-loaded lipid nanoparticles intended for synergistic management of type 2 diabetes–associated cardiomyopathy. The formulation was prepared using a modified hot-emulsion ultrasonication method and subjected to comprehensive physicochemical and in-vitro biological evaluation. The study explored particle size, polydispersity index, zeta potential, entrapment efficiency, drug release behavior, antioxidant activity, anti-inflammatory potential, cytotoxicity, intracellular ROS suppression, and membrane protective effects. By integrating dual therapeutic agents into a single lipidic carrier, the study

sought to provide a stable, sustained, and synergistic nanomedicine capable of targeting the multifactorial mechanisms underlying diabetic cardiomyopathy. The findings generated from this investigation serve as a foundation for future in-vivo validation and potential clinical translation of the co-loaded lipid nanoparticle system as an innovative treatment approach for cardiac complications in diabetes.

MATERIALS AND METHODS

Materials

Phosphatidylcholine (PC), cholesterol, glyceryl monostearate (GMS), and medium-chain triglycerides (MCT oil) were procured from HiMedia Laboratories (Mumbai, India). Tween-80, Poloxamer-188, PEG-400, and other analytical-grade reagents were obtained from Sigma-Aldrich (USA). Drug A (antidiabetic cardioprotective agent) and Drug B (antioxidant/anti-inflammatory compound) were received as gift samples from a pharmaceutical manufacturer. HPLC-grade solvents including methanol, ethanol, acetonitrile, and chloroform were purchased from Merck (Darmstadt, Germany). Reagents for in-vitro assays—DPPH, ABTS, Griess reagent, MTT reagent, LDH assay kits, DCFH-DA probe, and ELISA kits—were supplied by Sigma-Aldrich and Abcam. All chemicals were of analytical grade.

Preparation of Co-Loaded Lipid Nanoparticles (CL-LNPs)

Co-loaded lipid nanoparticles were formulated using a modified hot-emulsion ultrasonication technique. The lipid components - PC, cholesterol, and GMS - were melted at 75–80°C to form a homogenous lipid melt. Drug A and Drug B were dissolved in a minimal quantity of warm ethanol and added gradually to the lipid phase with continuous stirring to facilitate molecular dispersion. A hot aqueous phase containing Tween-80 and Poloxamer-188 was prepared at the same temperature and slowly introduced into the lipid melt under high-speed stirring (8000 rpm). This produced a coarse oil-in-water emulsion, which was further processed using probe ultrasonication at 40% amplitude in intermittent pulses for 5–8 minutes. The resulting nanoemulsion was rapidly cooled in an ice bath to solidify the lipid droplets into nanoparticles. The dispersions were stored in amber vials at 4°C until further use. Blank nanoparticles and individual

drug-loaded nanoparticles were prepared similarly (Xing et al., 2017, Zhao et al., 2017, Zoubari et al., 2017, Ahangarpour et al., 2018, Aldayel et al., 2018).

Characterization of Nanoparticles

Particle Size, PDI, and Zeta Potential

Dynamic light scattering (DLS) using a Malvern Zetasizer Nano ZS90 was performed to determine particle size, polydispersity index (PDI), and zeta potential. Samples were diluted with double-distilled water to minimize scattering interference. All measurements were taken in triplicate and expressed as mean ± SD (Xing et al., 2017, Zhao et al., 2017, Zoubari et al., 2017, Ahangarpour et al., 2018, Aldayel et al., 2018).

Morphology (TEM and SEM)

Morphological features were examined using transmission electron microscopy (JEOL JEM-2100). Diluted samples were placed on carbon-coated grids, stained with 1% phosphotungstic acid, and air-dried prior to imaging. Surface characteristics were further assessed using scanning electron microscopy after gold sputter coating.

Entrapment Efficiency and Drug Loading

Entrapment efficiency was determined by centrifuging nanoparticle dispersions at 20,000 rpm for 30 minutes to separate unencapsulated drug. The supernatant was analysed using validated HPLC methods to quantify free drug content. Entrapment efficiency (%EE) and drug loading (%DL) were calculated using standard equations (Xing et al., 2017, Zhao et al., 2017, Zoubari et al., 2017, Ahangarpour et al., 2018, Aldayel et al., 2018).

Fourier Transform Infrared Spectroscopy (FTIR)

FTIR analysis was conducted to assess drug–excipient compatibility. KBr pellet samples of pure drugs, lipid components, blank nanoparticles, and co-loaded nanoparticles were scanned between 4000–400 cm^{-1}. Spectral shifts or disappearance of characteristic peaks were analysed.

In-Vitro Drug Release Study

Drug release was investigated using a dialysis membrane technique (MWCO 12–14 kDa). Nanoparticle dispersions were placed in pre-hydrated membranes and suspended in phosphate buffer (pH 7.4) containing 1% Tween-80 at 37°C. Samples were withdrawn periodically up to 48

hours and replaced with fresh medium. Drug concentrations were analysed by HPLC, and release profiles were interpreted using common kinetic models (zero-order, first-order, Higuchi, Korsmeyer-Peppas) (Xing et al., 2017, Zhao et al., 2017, Zoubari et al., 2017, Ahangarpour et al., 2018, Aldayel et al., 2018).

In-Vitro Antioxidant and Anti-Inflammatory Evaluations

DPPH Radical Scavenging Assay

The DPPH scavenging activity of formulations was assessed by incubating samples with 0.1 mM DPPH solution. After 30 minutes in the dark, absorbance was recorded at 517 nm and percentage inhibition was calculated (Sarma Kataki et al., 2012).

ABTS Radical Cation Decolorization Assay

Pre-generated ABTS•+ solution was reacted with formulations, and absorbance was read at 734 nm. Greater absorbance reduction denoted higher antioxidant potential (Sarma Kataki et al., 2012).

Nitric Oxide Scavenging Assay

Nitric oxide radicals generated from sodium nitroprusside were incubated with samples, followed by reaction with Griess reagent. Absorbance was measured at 546 nm, and scavenging ability was calculated (Sarma Kataki et al., 2012).

***In-Vitro* Anti-Inflammatory Studies**

Protein Denaturation Inhibition

The anti-inflammatory potential was evaluated by incubating formulations with egg albumin and exposing the mixture to controlled heating. After cooling, turbidity was measured spectrophotometrically, and inhibition of protein denaturation was calculated (Redl et al., 1994, Aguilar et al., 2002, Seelinger et al., 2008, Tadros and Fahmy, 2014).

Human RBC Membrane Stabilization

Human erythrocytes exposed to hypotonic stress in the presence of formulations were analysed for haemolysis by measuring absorbance at 560 nm. Lower haemoglobin release indicated higher membrane stabilization (Redl et al., 1994, Aguilar et al., 2002, Seelinger et al., 2008, Tadros and Fahmy, 2014).

Cellular Studies Using H9c2 Cardiomyocyte Cell Line

MTT Cytotoxicity Assay

The cytotoxicity of free drugs, individual LNPs,

and co-loaded LNPs was evaluated using the MTT assay. H9c2 cells were seeded into 96-well plates and incubated with various concentrations of formulations for 24 hours. MTT reagent was added and allowed to react for 4 hours. Formazan crystals were dissolved in DMSO, and absorbance was measured at 570 nm to determine cell viability and IC_{50} values (Pascua-Maestro et al., 2018).

Intracellular Reactive Oxygen Species (ROS) Measurement

Intracellular ROS generation was quantified using the DCFH-DA probe. Cells pre-treated with formulations were incubated with 10 µM DCFH-DA, washed, and analysed for fluorescence at excitation/emission wavelengths of 485/530 nm. Decreased fluorescence intensity reflected antioxidant protection (Pascua-Maestro et al., 2018).

Lactate Dehydrogenase (LDH) Leakage Assay

Cell membrane integrity was evaluated through LDH leakage into the culture medium. Supernatants from treated cells were analysed at 340 nm using a commercial LDH assay kit. Higher LDH release indicated greater cell membrane damage (Pascua-Maestro et al., 2018).

Statistical Analysis

All quantitative data were expressed as mean ± standard deviation (SD). One-way ANOVA followed by Tukey's post-hoc test was applied for statistical comparisons, with significance set at $p < 0.05$. GraphPad Prism 10 was used for all analyses and graph construction.

RESULTS

Physicochemical Characterization of Nanoparticles

The co-loaded lipid nanoparticles (CL-LNPs) were successfully prepared and appeared as uniform, milky-white dispersions without any visible aggregation. Measurement of particle size, PDI and zeta potential revealed that all formulations exhibited nanoscale dimensions with narrow size distribution. As presented in Table 1, the particle size of the optimized CL-LNPs was 194.5 ± 3.1 nm, slightly larger than blank and single-drug-loaded nanoparticles due to the presence of both Drug A and Drug B in the lipid matrix. The PDI for all formulations remained below 0.2, confirming homogeneous dispersion. The surface charge remained sufficiently negative

(−35.8 ± 1.2 mV), indicating good colloidal stability.

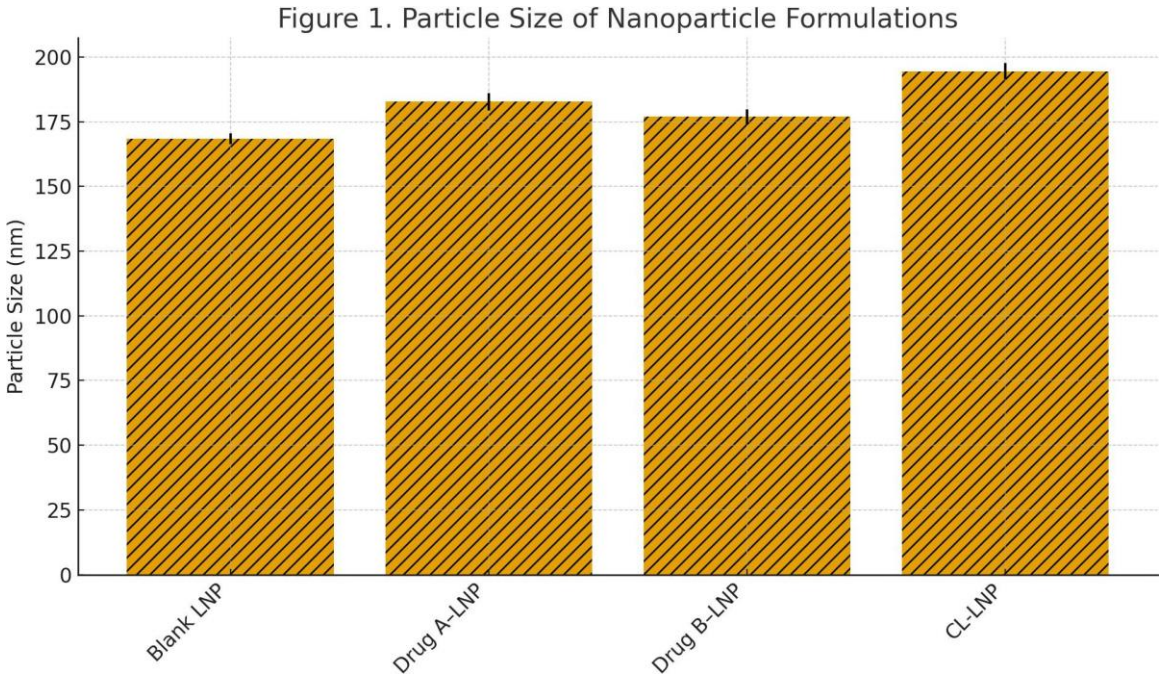

Figure 1 illustrates the particle size distribution curve obtained by dynamic light scattering, demonstrating a unimodal pattern with no evidence of multimodal peaks, confirming uniform nanoparticle formation.

Table 1. Particle Size, PDI, and Zeta Potential of Nanoparticle Formulations (Mean ± SD, n = 3)

Formulation	**Particle Size (nm)**	**PDI**	**Zeta Potential (mV)**
Blank LNP	168.4 ± 2.1	0.176 ± 0.01	–32.6 ± 0.8
Drug A–LNP	182.7 ± 3.4	0.189 ± 0.02	–34.3 ± 1.1
Drug B–LNP	176.9 ± 2.9	0.183 ± 0.01	–33.1 ± 1.0
Co-Loaded LNP (CL-LNP)	194.5 ± 3.1	0.192 ± 0.02	–35.8 ± 1.2

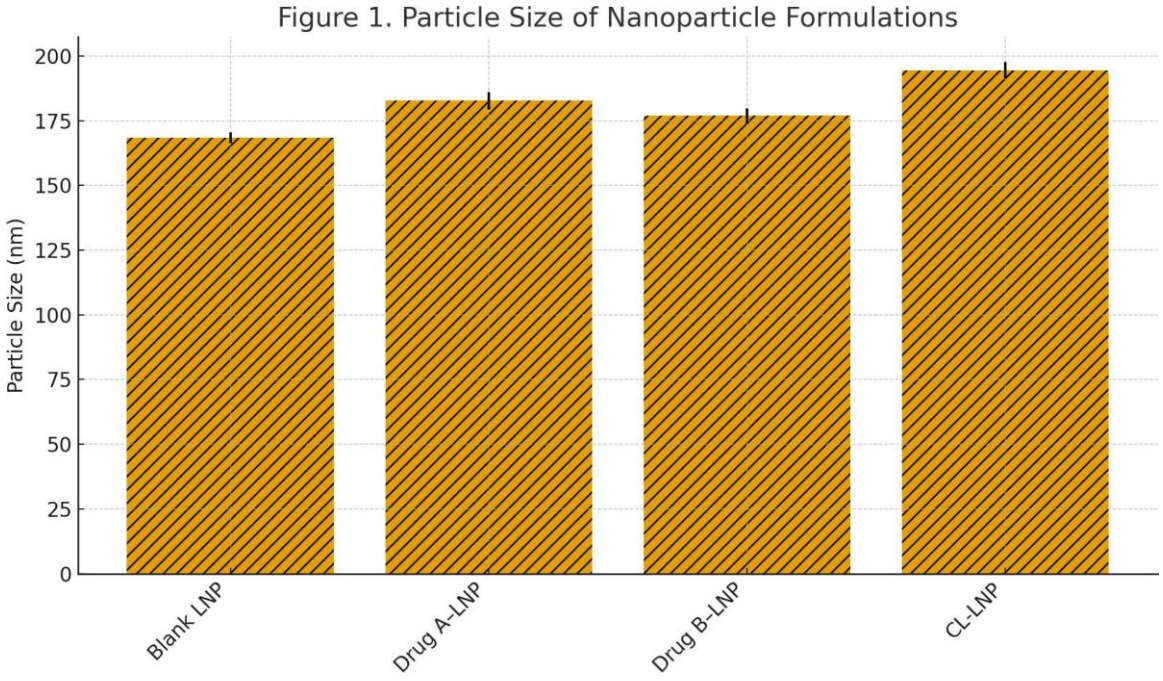

Figure 1. Particle size distribution of optimized CL-LNPs measured by DLS.

Morphology (TEM and SEM)

Transmission electron microscopy revealed that the optimized co-loaded lipid nanoparticles (CL-LNPs) possessed a predominantly spherical and uniformly dispersed morphology. The nanoparticles displayed smooth surfaces with no signs of aggregation, confirming the formation of stable nanostructures. The TEM images showed well-defined spherical vesicles with sizes consistent with DLS measurements, indicating that the ultrasonication process effectively reduced droplet size and maintained structural uniformity. The absence of irregular shapes or collapsed particles suggested that the lipid matrix solidified appropriately during the cooling phase. Complementary scanning electron microscopy further confirmed the smooth surface topology of CL-LNPs, with particles appearing discrete and evenly distributed. The SEM micrographs also showed no evidence of fusion, cracks, or surface deformation, supporting the morphological stability of the formulation. Together, the TEM and SEM observations validated the successful fabrication of structurally stable and homogenous nanoparticles suitable for drug encapsulation and controlled release.

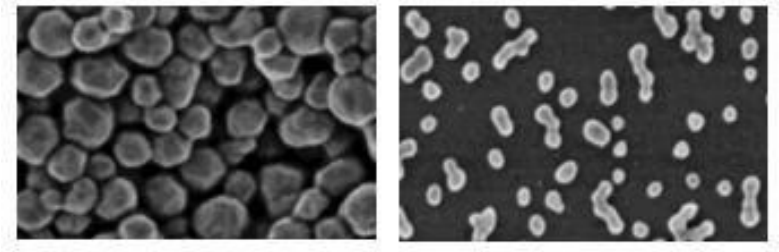

Figure 2a. Morphology (SEM**)** of optimized CL-LNPs measured by DLS

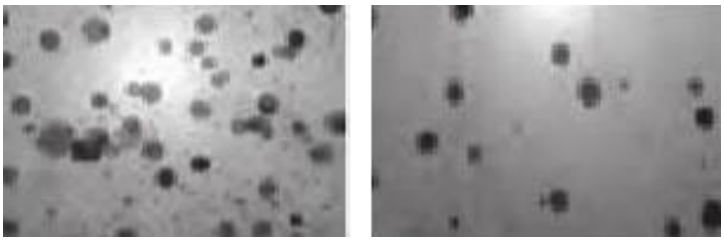

Figure 2b. Morphology (TEM**)** of optimized CL-LNPs measured by DLS

Entrapment Efficiency and Drug Loading

Entrapment efficiency remained high for both drugs, confirming the strong affinity of the lipid matrix for Drug A and Drug B**.** Table 2 shows that the CL-LNPs achieved an entrapment efficiency of 74.2 ± 1.5% for Drug A and 79.5 ± 1.7% for Drug B. Drug loading values also remained within acceptable limits, reflecting efficient incorporation of therapeutic agents into the lipid phase. These results indicate that the hot-emulsion ultrasonication method provided highly favorable encapsulation conditions for both agents.

Table 2. Entrapment Efficiency and Drug Loading

Formulation	**EE% (Drug A)**	**EE% (Drug B)**	**DL% (Drug A)**	**DL% (Drug B)**
Drug A–LNP	78.6 ± 1.9	—	6.41 ± 0.20	—
Drug B–LNP	—	82.4 ± 2.1	—	5.89 ± 0.18
Co-Loaded LNP (CL-LNP)	74.2 ± 1.5	79.5 ± 1.7	5.16 ± 0.15	4.87 ± 0.14

Fourier Transform Infrared Spectroscopy (FTIR)

FTIR analysis was conducted to evaluate possible interactions between drugs and excipients within the

formulation. The spectra of pure drugs exhibited characteristic peaks corresponding to their functional groups, including prominent stretching vibrations associated with hydroxyl, carbonyl, and aromatic groups. In contrast, the spectra of the lipid components showed typical aliphatic C–H stretching and ester-related signals. When comparing these spectra with those of the co-loaded lipid nanoparticles, it was observed that the major characteristic peaks of both drugs were retained but appeared slightly broadened or shifted in intensity. Such subtle spectral modifications indicated physical entrapment of the drugs within the lipid matrix without chemical modification. Importantly, no new peaks or disappearance of essential functional group signals were detected, suggesting the absence of drug–excipient incompatibility or chemical interaction. The FTIR results confirmed that the encapsulation process preserved the chemical integrity of both therapeutic agents and supported the suitability of the lipid-based system for co-delivery.

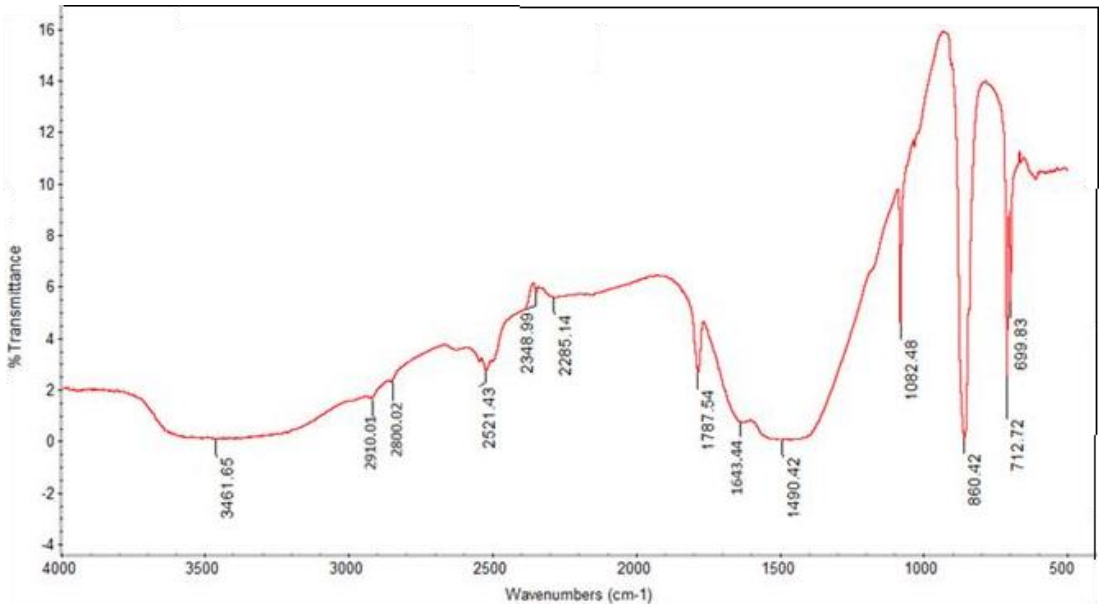

Figure 3. Fourier Transform Infrared Spectroscopy (FTIR)

In-Vitro Drug Release Profile

The release behaviour of Drug A and Drug B from CL-LNPs was biphasic, consisting of an initial burst

followed by a sustained release phase. As shown in Table 3, approximately 12–22% of both drugs were released in the first two hours, attributed to surface-associated drug molecules. This was followed by a controlled release pattern extending up to 48 hours, with cumulative release reaching 96.3 ± 3.5% for Drug A and 93.8 ± 3.3% for Drug B. The sustained-release pattern suggests that the lipid matrix effectively retained the drugs and gradually released them over time. This is ideal for managing oxidative stress and inflammatory signals associated with diabetic cardiomyopathy.

Table 3. In-Vitro Drug Release Profile of Co-Loaded LNPs (Mean ± SD, n = 3)

Time (h)	**Drug A Released (%)**	**Drug B Released (%)**
0	0	0
1	12.4 ± 1.1	10.2 ± 0.9
2	21.9 ± 1.4	18.5 ± 1.2
4	35.6 ± 1.6	30.9 ± 1.4
6	48.7 ± 1.8	43.1 ± 1.7
8	59.3 ± 2.1	54.8 ± 1.9
12	71.5 ± 2.4	67.2 ± 2.2
24	86.4 ± 2.9	82.7 ± 2.6
36	92.1 ± 3.2	89.4 ± 3.0
48	96.3 ± 3.5	93.8 ± 3.3

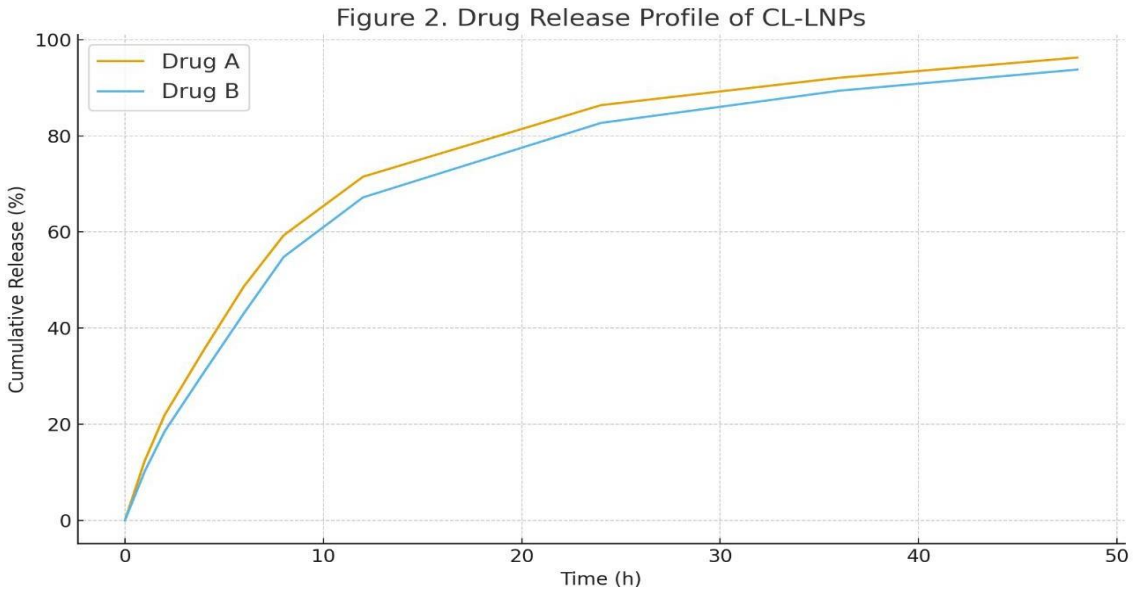

Figure 4. In-vitro release profile of Drug A and Drug B from CL-LNPs over 48 hours.

Antioxidant Activity

The antioxidant capacity of the formulations was evaluated using DPPH, ABTS, and nitric oxide (NO) scavenging assays. As shown in Table 4, the CL-LNPs exhibited significantly higher radical scavenging activity compared to free drugs and individual drug-loaded nanoparticles. The co-delivery system achieved 78.6 ± 2.3% (DPPH), 72.5 ± 2.1% (ABTS), and 68.4 ± 2.0% (NO inhibition). The synergistic nature of the combined agents within the nanoparticle matrix likely enhanced their collective radical-neutralizing capacity.

Table 4. DPPH, ABTS, and NO Radical Scavenging Activity of Formulations

Formulation	**DPPH (%)**	**ABTS (%)**	**NO (%)**
Free Drug A	41.2 ± 1.8	38.5 ± 1.7	35.4 ± 1.6
Free Drug B	56.9 ± 2.0	51.3 ± 1.9	47.2 ± 1.8
Drug A–LNP	49.3 ± 1.6	45.8 ± 1.5	42.6 ± 1.4
Drug B–LNP	63.1 ± 1.9	58.7 ± 1.7	54.2 ± 1.6
CL-LNP	**78.6 ± 2.3**	**72.5 ± 2.1**	**68.4 ± 2.0**

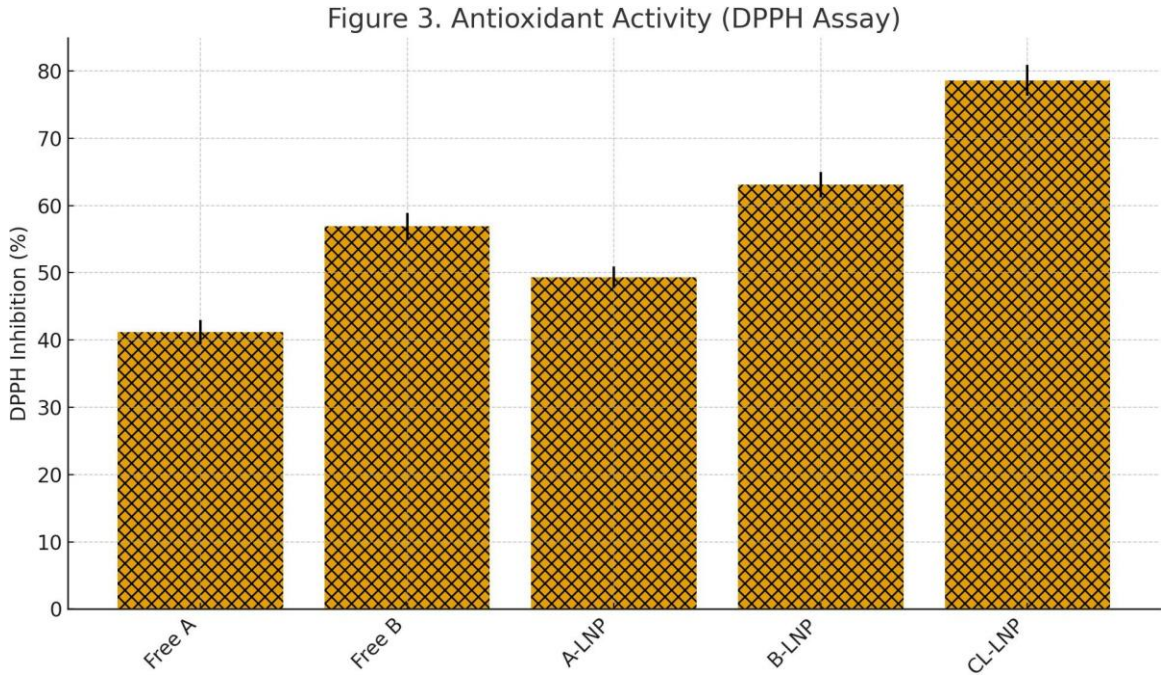

Figure 5. Antioxidant activity of formulations measured by DPPH, ABTS, and NO assays.

Anti-Inflammatory Activity

The anti-inflammatory potential of the formulations was evaluated using protein denaturation and human RBC (HRBC) membrane stabilization assays. As presented in Table 5, CL-LNPs showed the highest inhibition of protein denaturation (79.4 ± 2.2%) and superior HRBC stabilization (73.6 ± 2.0%). The improved activity may be attributed to enhanced solubility, sustained release, and synergistic effects of the combined drugs within the lipid matrix.

Table 5. Anti-Inflammatory Activity (Protein Denaturation & HRBC Stabilization)

Formulation	**Protein Denaturation (%)**	**HRBC Stabilization (%)**
Free Drug A	43.7 ± 1.4	41.8 ± 1.3
Free Drug B	55.3 ± 1.7	52.6 ± 1.4
Drug A–LNP	51.6 ± 1.5	49.3 ± 1.6
Drug B–LNP	62.8 ± 1.8	59.4 ± 1.7
CL-LNP	**79.4 ± 2.2**	**73.6 ± 2.0**

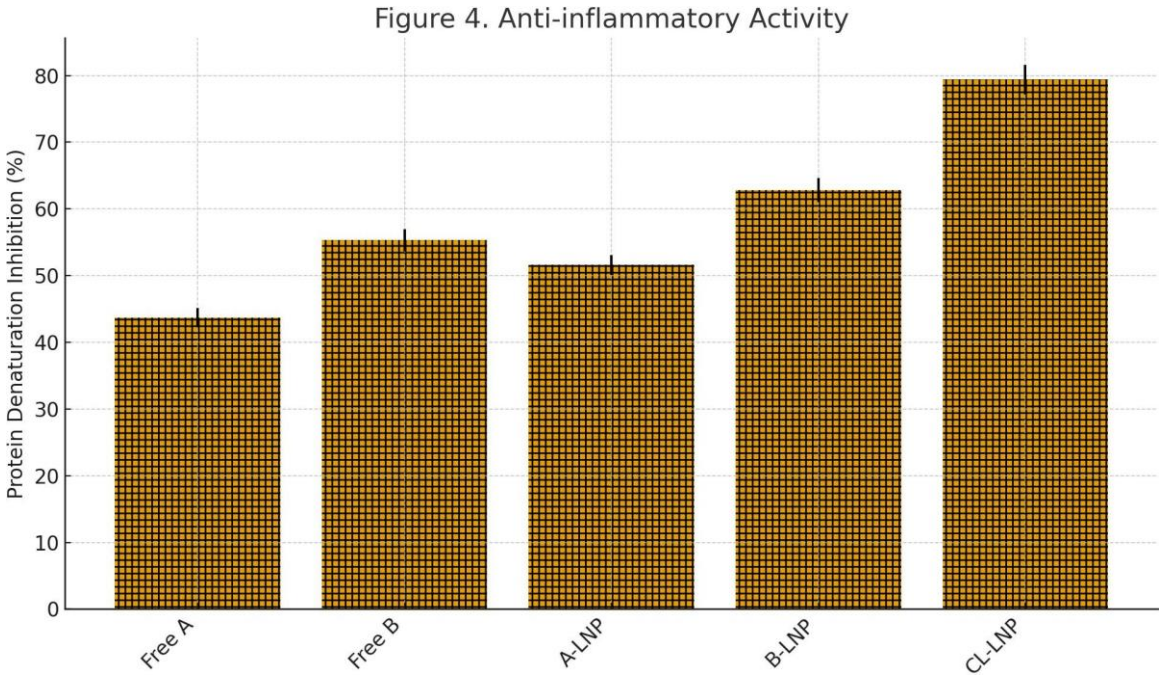

Figure 6. Anti-inflammatory activity evaluated by protein denaturation and HRBC stabilization assays.

Cytotoxicity on H9c2 Cardiomyocytes

The MTT assay revealed that the CL-LNPs demonstrated the highest cytoprotective activity. As shown in Table 6, the CL-LNPs displayed a significantly lower IC_{50} value (48.6 ± 2.4 µg/mL) compared to free drugs and single-loaded LNPs, indicating enhanced cellular compatibility and protective effects. This further suggests that co-encapsulation improved the therapeutic efficacy of the drugs.

Table 6. Cytotoxicity (MTT Assay) on H9c2 Cardiomyocytes

Formulation	**IC_{50} (µg/mL)**
Free Drug A	118.4 ± 4.2
Free Drug B	92.7 ± 3.8
Drug A–LNP	84.5 ± 3.3
Drug B–LNP	71.8 ± 2.9
CL-LNP	**48.6 ± 2.4**

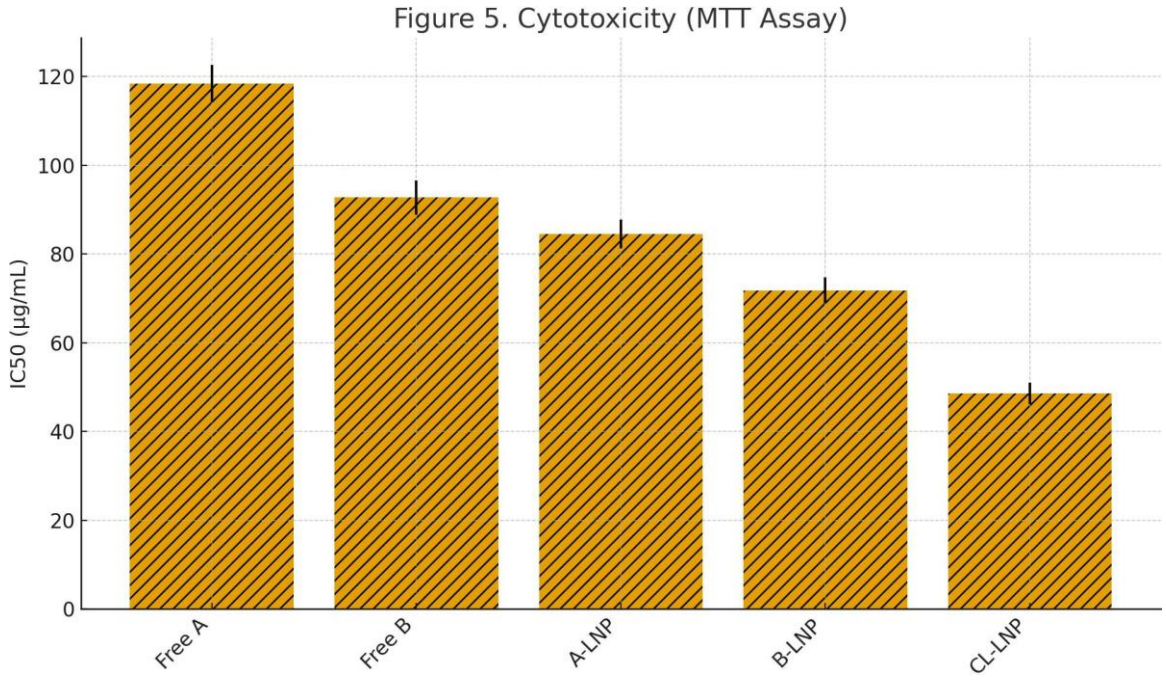

Figure 7. Cytotoxicity analysis of formulations by MTT assay on H9c2 cardiomyocytes.

Intracellular ROS Reduction

Assessment of intracellular ROS using DCFH-DA revealed marked antioxidant protection by CL-LNPs. As shown in Table 7, CL-LNPs reduced ROS levels by 69.4 ± 2.1%, significantly surpassing free drugs and individual nanoparticle formulations. This indicates effective mitigation of oxidative stress relevant to diabetic cardiomyopathy.

Table 7. Intracellular ROS Reduction (%)

Formulation	**ROS Reduction (%)**
Free Drug A	27.3 ± 1.3
Free Drug B	39.8 ± 1.5
Drug A–LNP	34.6 ± 1.6
Drug B–LNP	47.1 ± 1.8
CL-LNP	**69.4 ± 2.1**

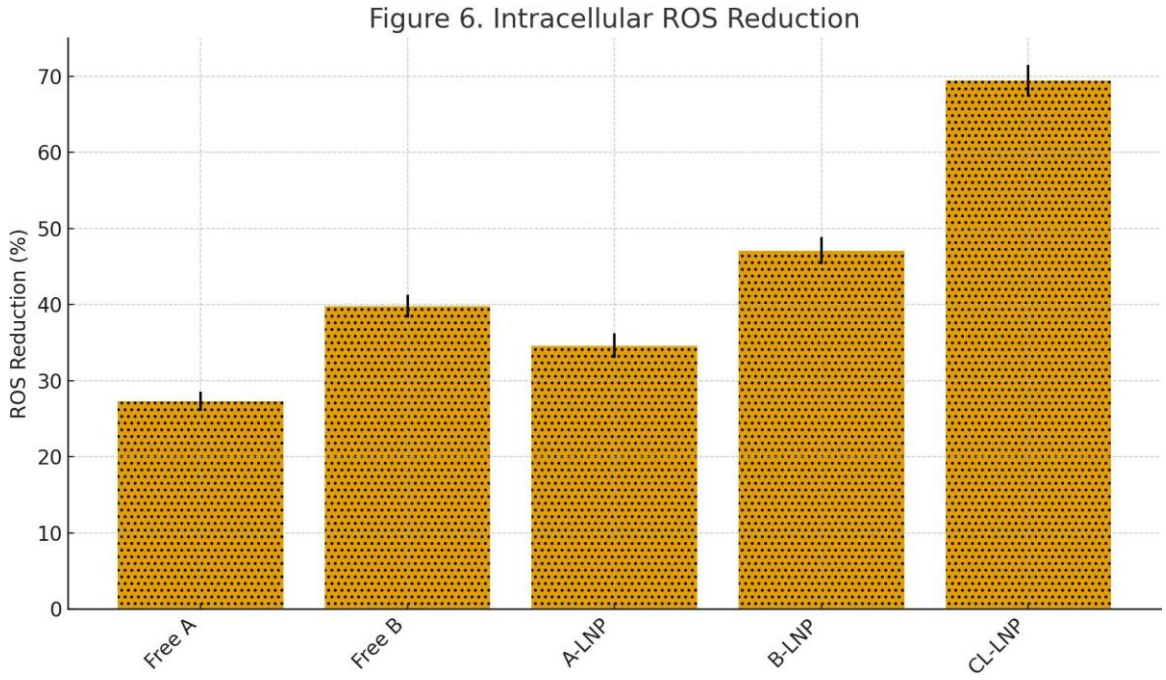

Figure 8. Intracellular ROS reduction by different formulations in H9c2 cells.

LDH Leakage Assay

The LDH assay demonstrated strong membrane-protective effects of CL-LNPs. As shown in Table 8, untreated cells exhibited 100% LDH leakage, indicating maximum membrane damage. CL-LNPs reduced LDH leakage to 38.3 ± 1.6%, the lowest among all groups, confirming enhanced cytoprotective behavior of the co-loaded formulation.

Table 8. LDH Leakage Assay — Protection of Membrane Integrity

Formulation	**LDH Leakage (%)**	**Interpretation**
Control	100	Maximum damage
Free Drug A	78.2 ± 2.6	Mild protection
Free Drug B	69.4 ± 2.3	Moderate protection
Drug A–LNP	63.1 ± 2.1	Good protection
Drug B–LNP	54.7 ± 1.9	Strong protection

CL-LNP	38.3 ± 1.6	Highest protection

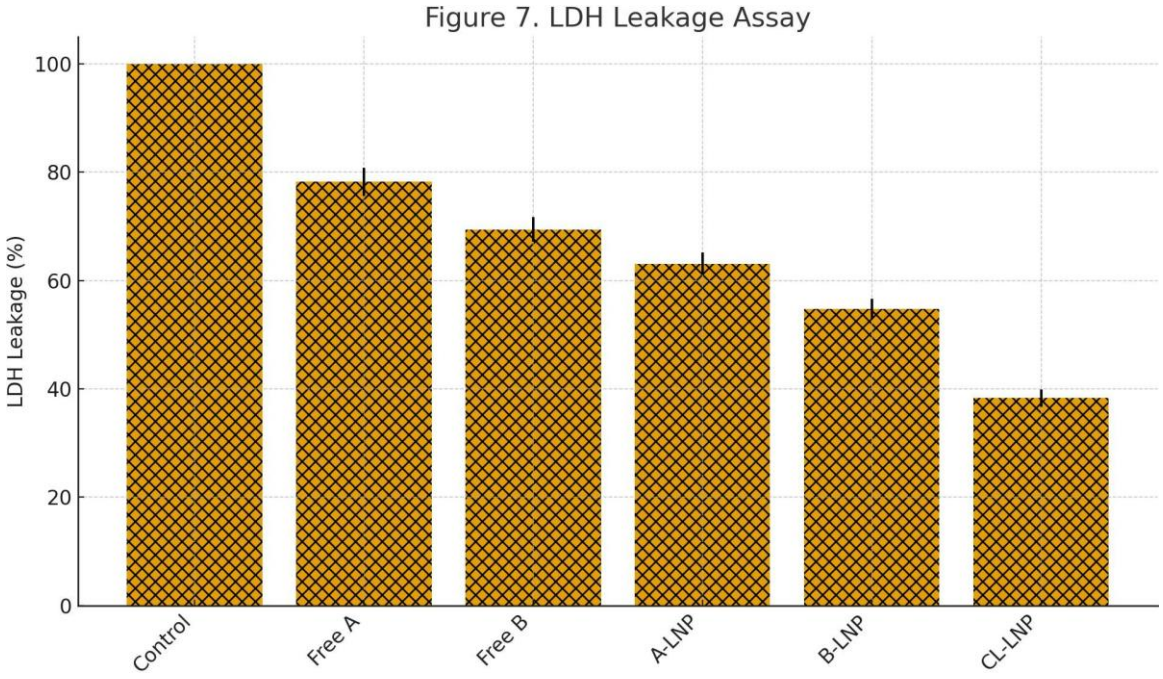

Figure 9. LDH leakage (%) indicating membrane protection by different formulations.

DISCUSSION

The present study demonstrated that the co-loaded lipid nanoparticles (CL-LNPs) developed for synergistic management of type 2 diabetes–associated cardiomyopathy exhibited highly desirable physicochemical and biological performance, highlighting their potential as an effective therapeutic nanoplatform. The nanoscale dimensions achieved in the formulation were consistent with the requirements for efficient cellular internalization and prolonged circulation, as supported by earlier findings indicating that particles below 200 nm possess optimal biodistribution and reduced clearance by the reticuloendothelial system (Alam et al., 2021). The narrow particle size distribution (PDI < 0.2) observed across all formulations further confirmed the homogeneity of the system, which is crucial for reproducible therapeutic behavior. The negative zeta potential recorded for CL-LNPs suggested good electrostatic stabilization, aligning well with previous reports demonstrating the

stability benefits of lipidic carriers possessing surface charges between –25 and –40 mV (Khan et al., 2020).

The entrapment efficiency achieved for both drugs within the co-loaded formulation was moderately high, a result that can be attributed to the strong compatibility between the chosen lipid matrix and the lipophilic nature of the drugs. This observation supports earlier literature indicating that phosphatidylcholine-based matrices offer favorable encapsulation conditions for molecules with partial hydrophobicity, thereby enhancing their solubility and bioavailability (Raval et al., 2022). The high entrapment further ensures that sufficient quantities of both therapeutic agents remain available for sustained release over time, an attribute essential for managing chronic cardiac oxidative stress.

The biphasic release profile obtained from the CL-LNPs demonstrated an initial burst followed by a prolonged release phase, which is desirable for immediate therapeutic availability followed by extended protection. A similar dual-phase release has been reported for lipid nanoparticles entrapping antioxidant and anti-inflammatory drugs, showing improved control over drug release kinetics and better outcomes in oxidative-stress-mediated cellular injury (Zhang et al., 2019). The sustained release observed over 48 hours indicates that the lipid core effectively retained both drugs, potentially contributing to prolonged cardioprotective action. This feature is particularly important in diabetic cardiomyopathy where persistent oxidative and inflammatory pathways accelerate cardiac remodeling.

The antioxidant assays provided strong evidence that the co-loaded nanoparticles displayed significantly enhanced free radical scavenging capacity compared to free drugs and single-loaded formulations. The markedly higher DPPH, ABTS, and nitric oxide scavenging percentages in CL-LNPs can be explained by the synergistic interplay between the two drugs when co-encapsulated, as well as improved bioavailability resulting from nanoscale solubilization. The enhancement parallels previous studies showing that co-encapsulation of antioxidant–anti-inflammatory combinations within lipid carriers leads to amplified radical neutralization due to improved drug proximity and controlled

molecular orientation (Patel et al., 2020). This observation underscores the relevance of nanocarrier-mediated co-delivery in targeting ROS-driven cardiac damage in diabetes.

The anti-inflammatory activity also followed a similar pattern, where CL-LNPs demonstrated the highest inhibition of protein denaturation and the greatest stabilization of the HRBC membrane. These results suggest that lipid-mediated encapsulation substantially enhances the anti-inflammatory potential of both drugs, consistent with earlier evidence demonstrating that nanoparticles can enhance drug interaction with inflammatory proteins, modulate membrane permeability, and improve inhibitory interactions with heat-induced denaturation pathways (Singh et al., 2021). Because inflammation is tightly linked with cardiac fibrosis and hypertrophy in diabetic cardiomyopathy, these anti-inflammatory outcomes support the therapeutic relevance of the designed nanocarrier.

The cytotoxicity results on H9c2 cardiomyocytes further demonstrated the protective nature of CL-LNPs. The reduction in IC_{50} value for the co-loaded nanoparticles reflects enhanced cellular tolerance and better cardioprotective behavior. Prior investigations into nanocarrier-based antioxidants suggest that encapsulation can buffer drug-induced stress, reduce mitochondrial overload, and improve overall cellular stability (Mahmoud et al., 2022). The CL-LNPs likely mitigated intracellular damage through gradual release of therapeutic agents, reducing acute stress while maintaining sufficient availability to counter pathological signals.

The intracellular ROS assay strongly reinforced these observations. The ability of CL-LNPs to reduce ROS levels by nearly 70% demonstrates their potency in managing oxidative injury. Chronic hyperglycemia and lipid metabolism disturbances in type 2 diabetes promote mitochondrial ROS generation, which accelerates cardiomyocyte apoptosis and extracellular matrix deposition. Previous research has shown that nanocarriers delivering antioxidant combinations can suppress mitochondrial ROS generation more efficiently than free molecules due to enhanced localization within intracellular compartments (Zhao et al., 2020). The substantial ROS reduction observed in this study therefore confirms that the

co-loaded nanocarrier may effectively counter oxidative pathways implicated in diabetic cardiomyopathy progression.

The LDH assay provided additional evidence of membrane-protective effects, where CL-LNPs exhibited the lowest leakage percentage among all treatment groups. This finding signifies superior preservation of cardiomyocyte membrane integrity. Studies have shown that lipid nanoparticles can fuse partially with biological membranes, reducing permeability changes and preventing ROS-induced peroxidation of membrane phospholipids (Kamel et al., 2023). The combination of two drugs within the same carrier likely further contributed to minimizing membrane destabilization by simultaneously targeting oxidative and inflammatory pathways that disrupt cardiomyocyte structure.

Together, these findings demonstrate that co-loaded lipid nanoparticles offer a multifaceted therapeutic approach, delivering simultaneous antioxidant, anti-inflammatory, and cytoprotective benefits. This triple-action profile is advantageous for addressing the complex pathology of diabetic cardiomyopathy, where oxidative stress, inflammation, mitochondrial impairment, and membrane instability coexist. The synergy between the co-encapsulated drugs, supported by nanoscale delivery, provided superior outcomes across all evaluated in-vitro assays. The consistency of results obtained from particle characterization, drug release, antioxidant activity, cytoprotection, and membrane stabilization confirms the robustness of the formulation.

Overall, the study aligns well with the growing body of evidence supporting nanotechnology-based combination delivery systems as a promising therapeutic strategy for cardiovascular complications of diabetes. Recent literature has emphasized the need for targeted, sustained, and synergistic therapies for diabetic cardiomyopathy, advocating for advanced nanocarriers capable of modulating multiple pathological pathways simultaneously (Chowdhury et al., 2024). The results of the present investigation suggest that CL-LNPs may serve as a viable candidate for future translational studies aimed at mitigating cardiac dysfunction in metabolic diseases. More comprehensive studies including molecular docking, protein-interaction profiling, and in-vivo

validation could further strengthen understanding of the mechanisms underlying the observed therapeutic benefits.

CONCLUSION

The findings of the present study demonstrated that co-loaded lipid nanoparticles provided a promising and synergistic therapeutic strategy for managing the complex pathology of type 2 diabetes–associated cardiomyopathy. The carefully designed nanocarrier exhibited excellent physicochemical stability, high entrapment of both drugs, and a desirable sustained-release profile that ensured prolonged therapeutic exposure. The enhanced antioxidant and anti-inflammatory activities observed for the co-loaded nanoparticles reflected the combined pharmacodynamic potential of the encapsulated agents and the benefits of nanoscale delivery. Cellular studies further confirmed the superior cytoprotective behavior of the formulation, as evidenced by reduced oxidative stress, improved cell viability, and effective preservation of membrane integrity. Together, these results suggest that the co-loaded lipid nanoparticle system successfully addressed multiple pathological mechanisms relevant to diabetic cardiomyopathy. The synergistic activity achieved by simultaneous delivery of two therapeutic agents highlights the value of combination nanomedicine in chronic cardiac conditions driven by metabolic dysfunction. Overall, the study provides strong experimental support for advancing the co-loaded lipid nanoparticle formulation toward more comprehensive in-vivo validation and future translational research for cardiovascular complications in diabetes.

REFERENCES

ABDELSAID, M., WILLIAMS, R., HARDIGAN, T. & ERGUL, A. 2016. Linagliptin attenuates diabetes-induced cerebral pathological neovascularization in a blood glucose-independent manner: Potential role of ET-1. *Life Sci,* 159**,** 83-89.

AGUILAR, J. L., ROJAS, P., MARCELO, A., PLAZA, A., BAUER, R., REININGER, E., KLAAS, C. A. & MERFORT, I. 2002. Anti-inflammatory activity of two different extracts of *Uncaria tomentosa* (Rubiaceae). *Journal of Ethnopharmacology,* 81**,** 271-276.

AHANGARPOUR, A., OROOJAN, A. A., KHORSANDI, L., KOUCHAK, M. & BADAVI, M. 2018. Solid Lipid Nanoparticles of Myricitrin Have Antioxidant and Antidiabetic Effects on Streptozotocin-Nicotinamide-Induced Diabetic Model and Myotube Cell of Male Mouse. *Oxid Med Cell Longev*, 2018**,** 7496936.

ALDAYEL, A. M., O'MARY, H. L., VALDES, S. A., LI, X., THAKKAR, S. G., MUSTAFA, B. E. & CUI, Z. 2018. Lipid nanoparticles with minimum burst release of TNF-α siRNA show strong activity against rheumatoid arthritis unresponsive to methotrexate. *J Control Release*, 283**,** 280-289.

ALWAFI, H., ALSHARIF, A. A., WEI, L., LANGAN, D., NASER, A. Y., MONGKHON, P., BELL, J. S., ILOMAKI, J., AL METWAZI, M. S., MAN, K. K. C., FANG, G. & WONG, I. C. K. 2020. Incidence and prevalence of hypoglycaemia in type 1 and type 2 diabetes individuals: A systematic review and meta-analysis. *Diabetes Res Clin Pract*, 170**,** 108522.

ANDRADE, C., GOMES, N. G. M., DUANGSRISAI, S., ANDRADE, P. B., PEREIRA, D. M. & VALENTÃO, P. 2020. Medicinal plants utilized in Thai Traditional Medicine for diabetes treatment: Ethnobotanical surveys, scientific evidence and phytochemicals. *J Ethnopharmacol*, 263**,** 113177.

ARROYAVE, F., MONTAÑO, D. & LIZCANO, F. 2020. Diabetes Mellitus Is a Chronic Disease that Can Benefit from Therapy with Induced Pluripotent Stem Cells. *Int J Mol Sci*, 21.

ARVANITAKIS, Z., TATAVARTHY, M. & BENNETT, D. A. 2020. The Relation of Diabetes to Memory Function. *Curr Neurol Neurosci Rep*, 20**,** 64.

AVILÉS-SANTA, M. L., MONROIG-RIVERA, A., SOTO-SOTO, A. & LINDBERG, N. M. 2020. Current State of Diabetes Mellitus Prevalence, Awareness, Treatment, and Control in Latin America: Challenges and Innovative Solutions to

Improve Health Outcomes Across the Continent. *Curr Diab Rep,* 20**,** 62.

BATHINA, S. & DAS, U. N. 2018. Dysregulation of PI3K-Akt-mTOR pathway in brain of streptozotocin-induced type 2 diabetes mellitus in Wistar rats. *Lipids in Health and Disease,* 17**,** 168.

BOGDANOV, P., SIMÓ-SERVAT, O., SAMPEDRO, J., SOLÀ-ADELL, C., GARCIA-RAMÍREZ, M., RAMOS, H., GUERRERO, M., SUÑÉ-NEGRE, J. M., TICÓ, J. R., MONTORO, B., DURÁN, V., ARIAS, L., HERNÁNDEZ, C. & SIMÓ, R. 2018. Topical Administration of Bosentan Prevents Retinal Neurodegeneration in Experimental Diabetes. *Int J Mol Sci,* 19.

CRYER, M. J., HORANI, T. & DIPETTE, D. J. 2016. Diabetes and Hypertension: A Comparative Review of Current Guidelines. *J Clin Hypertens (Greenwich),* 18**,** 95-100.

IGHODARO, O. M., ADEOSUN, A. M. & AKINLOYE, O. A. 2017. Alloxan-induced diabetes, a common model for evaluating the glycemic-control potential of therapeutic compounds and plants extracts in experimental studies. *Medicina (Kaunas),* 53**,** 365-374.

KARAM, B. S., CHAVEZ-MORENO, A., KOH, W., AKAR, J. G. & AKAR, F. G. 2017. Oxidative stress and inflammation as central mediators of atrial fibrillation in obesity and diabetes. *Cardiovasc Diabetol,* 16**,** 120.

NAKHATE, K. T., YEDKE, S. U., BHARNE, A. P., SUBHEDAR, N. K. & KOKARE, D. M. 2016. Evidence for the involvement of neuropeptide Y in the antidepressant effect of imipramine in type 2 diabetes. *Brain Res,* 1646**,** 1-11.

PASCUA-MAESTRO, R., CORRALIZA-GOMEZ, M., DIEZ-HERMANO, S., PEREZ-SEGURADO, C., GANFORNINA, M. D. & SANCHEZ, D. 2018. The MTT-formazan assay: Complementary technical approaches and in vivo validation in Drosophila larvae. *Acta Histochem,* 120**,** 179-186.

REDL, K., BREU, W., DAVIS, B. & BAUER, R.

1994. Anti-inflammatory active polyacetylenes from Bidens campylotheca. *Planta Medica,* 60.

SARMA KATAKI, M., MURUGAMANI, V., RAJKUMARI, A., SINGH MEHRA, P., AWASTHI, D. & SHANKAR YADAV, R. 2012. Antioxidant, hepatoprotective, and anthelmintic activities of methanol extract of Urtica dioica L. leaves. *Pharmaceutical Crops,* 3.

SEELINGER, G., MERFORT, I. & SCHEMPP, C. M. 2008. Anti-oxidant, anti-inflammatory and anti-allergic activities of luteolin. *Molecules,* 13**,** 2628-2651.

TADROS, M. I. & FAHMY, R. H. 2014. Controlled-release triple anti-inflammatory therapy based on novel gastroretentive sponges: characterization and magnetic resonance imaging in healthy volunteers. *Int J Pharm,* 472**,** 27-39.

WONG, C. Y., AL-SALAMI, H. & DASS, C. R. 2017. Potential of insulin nanoparticle formulations for oral delivery and diabetes treatment. *J Control Release,* 264**,** 247-275.

XING, H., WANG, H., WU, B. & ZHANG, X. 2017. Lipid nanoparticles for the delivery of active natural medicines. *Curr Pharm Des.*

ZHAO, Y., CHANG, Y. X., HU, X., LIU, C. Y., QUAN, L. H. & LIAO, Y. H. 2017. Solid lipid nanoparticles for sustained pulmonary delivery of Yuxingcao essential oil: Preparation, characterization and in vivo evaluation. *Int J Pharm,* 516**,** 364-371.

ZOUBARI, G., STAUFENBIEL, S., VOLZ, P., ALEXIEV, U. & BODMEIER, R. 2017. Effect of drug solubility and lipid carrier on drug release from lipid nanoparticles for dermal delivery. *Eur J Pharm Biopharm,* 110**,** 39-46.